


**Measurement of the conduction band spin-orbit splitting in WSe<sub>2</sub> and WS<sub>2</sub> monolayers**Lei Ren,<sup>1,\*</sup> Cedric Robert,<sup>1,\*</sup> Hanan Dery,<sup>2,3,\*</sup> Minhao He,<sup>4</sup> Pengke Li,<sup>2</sup> Dinh Van Tuan,<sup>2</sup> Pierre Renucci,<sup>1</sup> Delphine Lagarde,<sup>1</sup> Takashi Taniguchi,<sup>5</sup> Kenji Watanabe,<sup>6</sup> Xiaodong Xu,<sup>4,7</sup> and Xavier Marie<sup>1,†</sup><sup>1</sup>*Université de Toulouse, INSA-CNRS-UPS, LPCNO, 135 Avenue Rangueil, 31077 Toulouse, France*<sup>2</sup>*Department of Electrical and Computer Engineering, University of Rochester, Rochester, New York 14627, USA*<sup>3</sup>*Department of Physics and Astronomy, University of Rochester, Rochester, New York 14627, USA*<sup>4</sup>*Department of Physics, University of Washington, Seattle, Washington 98195, USA*<sup>5</sup>*International Center for Materials Nanoarchitectonics, National Institute for Materials Science, Tsukuba, Ibaraki 305-0044, Japan*<sup>6</sup>*Research Center for Functional Materials, National Institute for Materials Science, Tsukuba, Ibaraki 305-0044, Japan*<sup>7</sup>*Department of Materials Science and Engineering, University of Washington, Seattle, Washington 98195, USA* (Received 3 April 2023; revised 15 May 2023; accepted 17 May 2023; published 6 June 2023)

We have investigated charge tunable devices based on WSe<sub>2</sub> and WS<sub>2</sub> monolayers encapsulated in hexagonal boron nitride. In addition to the well-known radiative recombination of neutral and charged excitons, stationary photoluminescence measurements highlight a weaker-intensity optical transition that appears when the monolayer is electrostatically doped with electrons. We have carried out a detailed characterization of this photoluminescence line based on its doping dependence, its variation as a function of the optical excitation power, its polarization characteristics, and its *g* factor measured under longitudinal magnetic field. We interpret this luminescence peak as an impurity-assisted radiative recombination of the intervalley negatively charged exciton (triplet trion). In addition to the standard direct recombination, the triplet trion has a second recombination channel triggered by elastic scattering off the short-range impurity potential. The energy difference between the emitted photons from these two possible recombination processes of the same triplet trion is simply the single-particle conduction band spin-orbit splitting  $\Delta_c$ . We measure  $\Delta_c = 12 \pm 0.5$  meV for the WSe<sub>2</sub> monolayer and  $\Delta_c = 12 \pm 1$  meV for the WS<sub>2</sub> monolayer. These results demonstrate the importance of second-order exciton recombination processes in transition-metal dichalcogenide structures.

DOI: [10.1103/PhysRevB.107.245407](https://doi.org/10.1103/PhysRevB.107.245407)**I. INTRODUCTION**

Atomically thin layers of semiconductor transition-metal dichalcogenides (TMDs) open up new possibilities for investigating two-dimensional (2D) physics and for potential new applications [1–5]. The band structure is rather unique as a consequence of the large spin-orbit coupling and lack of crystal inversion symmetry of the hexagonal lattice [6]. In addition to the well-known large spin-orbit splitting of the valence bands (VB), the interplay between inversion asymmetry and spin-orbit interaction also yields a smaller spin splitting between the two lowest energy conduction bands (CBs) in the *K* valley  $\Delta_c$  [7]. Although this CB spin-orbit splitting has a strong impact on optical, transport, and spin-valley properties of TMD monolayers (MLs) [8,9], its exact value is still poorly known and highly debated. It has been calculated by various groups using *ab initio* techniques, yielding scattered results that range from  $\Delta_c = -4$  to 40 meV in WSe<sub>2</sub> monolayers [10–12].

From an experimental point of view, optical properties of TMD MLs are dominated by tightly bound excitons [3]. As a consequence, it is not straightforward to determine the single-particle CB spin-orbit splitting from the exciton

spectra. Bright and dark neutral excitons are formed with electrons occupying two different CBs with opposite spins in a given *K* valley. Yet the measurement of the splitting between these optically active and inactive excitons does not make it possible to determine  $\Delta_c$ . The reason is that in addition to this spin-orbit splitting, the energy difference between bright and dark excitons depends on the short-range electron-hole exchange interaction and the difference in binding energy of the two excitons formed with different electron effective masses [8,13,14]. The value of  $\Delta_c$  in a WSe<sub>2</sub> ML was estimated recently with an elegant method based on the measurement of the Rydberg series of bright and dark exciton states in a large in-plane magnetic field [15]. Other values of  $\Delta_c$  were extracted from transport and optical magnetospectroscopy measurements [16–20], showing scattered results that are influenced by many-body and band-gap renormalization effects in electron- or hole-rich MLs. A direct and accurate determination of  $\Delta_c$  is thus highly desirable.

In this work, thanks to the identification of a different line in the photoluminescence (PL) spectra of slightly electron-doped WSe<sub>2</sub> and WS<sub>2</sub> MLs, we straightforwardly measure  $\Delta_c = 12 \pm 0.5$  meV in WSe<sub>2</sub> ML and  $\Delta_c = 12 \pm 1$  meV in WS<sub>2</sub> ML. The PL line we evidenced is interpreted as an impurity-assisted recombination of the intervalley negatively charged exciton (triplet trion), whose radiative recombination energy differs by  $\Delta_c$  from that of the trion's direct optically active recombination. The organization of this paper is as

\*These authors contributed equally to this work.

†marie@insa-toulouse.fr

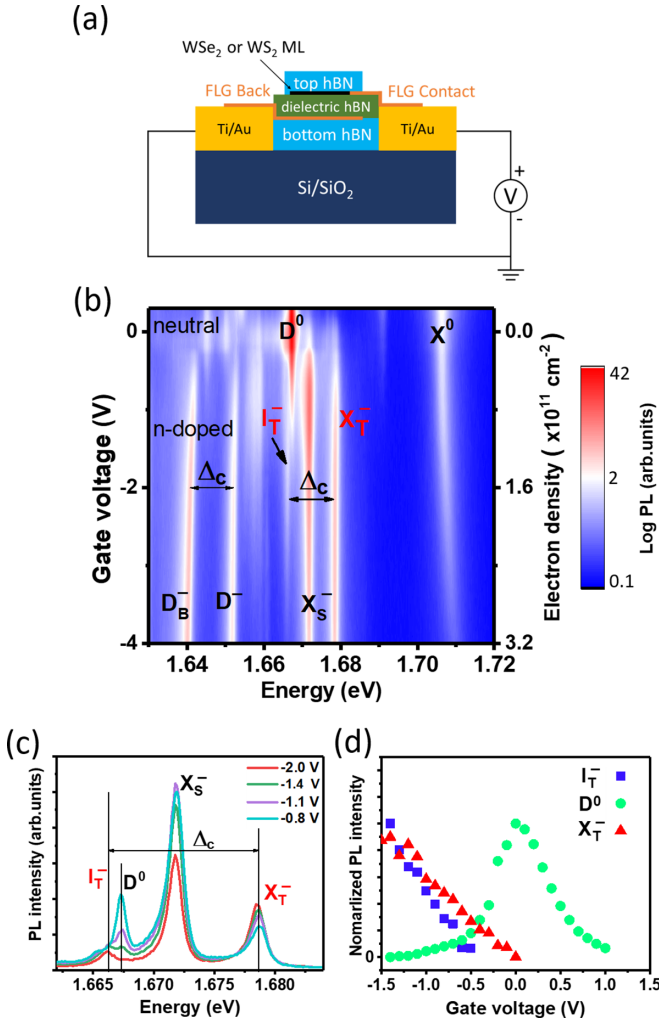


FIG. 1. (a) Sketch of the investigated devices with few-layer graphene (FLG) contacts. (b) Photoluminescence intensity in a WSe<sub>2</sub> monolayer as a function of gate voltage (left axis) and the corresponding electron density (right axis). The excitation energy is 1.96 eV.  $\Delta_c$  is the single-particle conduction band spin-orbit splitting. In addition to the relatively weak PL intensity of the peak  $I_T^-$ , the spectrum is dominated by emissions from bright and dark neutral excitons ( $X^0$  and  $D^0$ ), singlet and triplet bright negative trions ( $X_S^-$  and  $X_T^-$ ), and the dark negative trion along with its brightened component ( $D^-$  and  $D_B^-$ ) [8]. (c) The luminescence spectrum at various gate voltages. (d) Voltage dependence of the normalized luminescence intensity for the direct emission from  $D^0$ ,  $X_T^-$ , and  $I_T^-$ .

follows. The sample preparation and PL and magneto-PL measurements are described in Sec. II. Interpretation of the results based on the impurity-assisted recombination mechanism is presented in Sec. III, where we explain the radiative process and detail how to extract  $\Delta_c$ . Conclusions are given in Sec. IV, and the Supplemental Material includes complementary measurement results.

## II. EXPERIMENTS

We fabricated high-quality WSe<sub>2</sub> and WS<sub>2</sub> charge adjustable devices as sketched in Fig. 1(a). Details of sample fabrication can be found in Refs. [21,22]. Electrostatic dop-

ing of the ML is controlled by the voltage bias between the back gate and the ML. In the regime of slight to moderate electron density in the ML, the electrons populate only the lowest CBs in both the  $K^+$  and  $K^-$  valleys (see Fig. 2). A voltage bias change of 1 V in Fig. 1 typically corresponds to an electron density change of  $10^{11} \text{ cm}^{-2}$  [21]. As shown in Fig. S1 of the Supplemental Material [23], the measurements were also performed in another WSe<sub>2</sub> device described in Ref. [24]. Note that in the low-doping regime we consider here, the three-particle picture (i.e., trion) and the Fermi-polaron description are equivalent [25,26]. Continuous-wave polarization-dependent micro-PL experiments are performed in close cycle cryostats ( $T = 4 \text{ K}$ ). For WSe<sub>2</sub> and WS<sub>2</sub> devices, the excitation laser wavelengths are 632.8 and 532 nm, respectively. The PL signal is dispersed by a monochromator and detected by a charged-coupled device camera. Magneto-PL experiments in magnetic fields up to 9 T were carried out using an ultrastable home-made confocal microscope [27]. Unless otherwise stated, the excitation power is  $\sim 5 \mu\text{W}$ , focused to a spot size of  $\sim 1 \mu\text{m}$  diameter.

Three charge tunable WSe<sub>2</sub> devices were fabricated and investigated. As shown in the Supplemental Material, similar results were obtained, and here, we present the results for one of them. Figure 1(b) presents the PL intensity color plot as a function of applied voltage. In agreement with previous reports, the PL spectra are dominated by the recombination of bright ( $X^0$ ) and dark ( $D^0$ ) excitons in the charge-neutral regime (see Fig. S2 of the Supplemental Material [23]; the smaller intensity peaks at lower energy correspond to phonon replica [24,28]). When electrons are added to the ML (negative voltage in our notation), we observe the well-identified intravalley (singlet)  $X_S^-$  and intervalley (triplet)  $X_T^-$  negatively charged excitons (trions), composed of two electrons and one hole [29]. As shown in Fig. 2(a), the triplet trion is composed of a photogenerated electron-hole pair, made of an electron in the top CB and a missing electron in the topmost VB of the same valley, and the pair is bound to a resident electron in the bottom CB of the time-reversed valley. The dark trion ( $D^-$ ) can also be detected in Fig. 1(b) at lower energy [30–33]. The full width at half maximum of  $X^0$  at the charge neutrality point is only 2.5 meV, indicating the high quality of the sample.

A careful reading of Figs. 1(b) and 1(c) shows that a different line with a rather weak PL intensity appears at 1.666 eV for small negative voltages. This line, labeled  $I_T^-$  in the following, is spectrally resolved from the nearby dark exciton ( $D^0$ ), whose intensity dominates the spectrum when the ML is charge neutral. This PL component ( $I_T^-$ ) has not been identified so far, but it is present in the PL spectra measured independently by other groups on charge adjustable WSe<sub>2</sub> ML devices [24,34]. We have performed different characterizations in order to identify the origin of this PL peak.

Figure 1(d) displays the voltage dependence of the normalized PL intensity of line  $I_T^-$ , as well as the triplet trion ( $X_T^-$ ) and the neutral dark exciton ( $D^0$ ). It is clear that this line emerges when electrons are injected into the ML, while it does not appear when the ML is charge neutral (i.e., when the bright and dark exciton populations dominate). The increase in PL intensity of  $I_T^-$  when the electron density increases is very similar to the increase in emission intensity from the triplet trion ( $X_T^-$ ). With this simple measurement, we already can

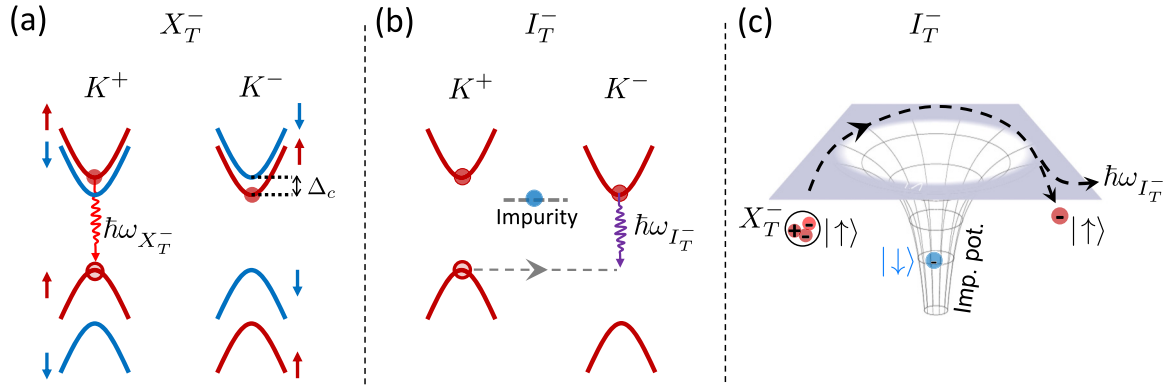


FIG. 2. (a) State composition of the triplet trion in  $k$  space. The initial trion energy is converted to an emitted photon  $\hbar\omega_{X_T^-}$  and an electron in the bottom valley of  $K^-$ . (b) The impurity-assisted recombination process for a triplet trion with spin-up electrons. The hole is transferred to the opposite valley following short-range interaction with the impurity, leading to radiative recombination of the hole with the “wrong” electron of the trion (i.e., the electron from the opposite valley). The “horizontal” intervalley transition of the hole represents the elastic nature of the impurity scattering. Using the language of second-order perturbation theory, upon spin-conserving scattering off the impurity, the hole is virtually transferred to the bottom valley of the VB in  $K^-$ , from which there is a strong in-plane dipole transition with the CB bottom valley at  $K^-$ . The initial trion energy is converted to the emitted photon energy  $\hbar\omega_{I_T^-}$  and the left-behind electron in the top valley of  $K^+$ . (c) Schematics of the radiative process in real space. A delocalized triplet trion with two spin-up electrons scatters off an impurity with spin-down localized electron, during which the hole recombines with one of the electrons in the trion. The antiparallel spin configuration of the electrons in the trion and impurity allows the trion to touch the impurity, whereas a parallel configuration is forbidden by Pauli exclusion.

infer that this line is linked to the recombination of a charged exciton species.

The PL intensity of this line depends linearly on the excitation power in the typical range between 0.05 and 5  $\mu\text{W}$  (see Figs. S3 and S5 of the Supplemental Material [23]). An interpretation based on multiple exciton complexes, such as a charged or neutral biexciton, or localized quantum-dot-like states can be ruled out because emissions from such states exhibit strongly nonlinear behaviors [35–38]. In addition, it turns out that the emission of this line is in plane polarized. Following the approach detailed in Ref. [39], we selectively filtered the emitted light in angle by imaging the Fourier plane of the microscope objective and by placing a pinhole on this image (Fig. S4 of the Supplemental Material [23]). We find that the emission from  $I_T^-$  is not  $z$  polarized, as opposed to the recombination of dark excitons or trions [32,39].

A decisive argument to identify PL line  $I_T^-$  is given by magneto-PL measurements presented in Figs. 3(a) and 3(b). We have recorded the right ( $\sigma^+$ ) and left ( $\sigma^-$ ) circularly polarized luminescence spectra for a magnetic field varying between  $B = -9$  and  $+9$  T, applied perpendicularly to the ML plane. The excitation laser is linearly polarized, and the gate voltage is  $-2$  V. Absorption or emission of  $\sigma^\pm$  light occurs in the inequivalent valleys at  $K^\pm$  in the 2D hexagonal Brillouin zone as a consequence of the interplay between spin-orbit interaction and the lack of inversion symmetry [6,40–43]. The  $g$  factor of a given optical transition with in-plane dipole is simply written as  $E_{\sigma^+} - E_{\sigma^-} = g\mu_B B$ , where  $\mu_B$  is the Bohr magneton. As already measured by different groups, we find very similar  $g$  factors for both neutral and negatively charged excitons:  $g_{X^0} = -4.1 \pm 0.1$ ,  $g_{X_T^-} = -4.4 \pm 0.1$ , and  $g_{X_S^-} = -4.2 \pm 0.1$  [22,44–49]. This can be explained by the fact that the optical recombination of these trions involves the same charge carriers in the same valley as for the recombination of the bright neutral exciton, while the spin/valley state of the

third carrier in the bottom CB valley is not changed [see, for instance, Fig. 2(a) for the  $X_T^-$  triplet trion recombination].

The striking feature in Fig. 3 is that the slope of the magnetic-field-dependent  $I_T^-$  line is opposite to that of the neutral exciton  $X^0$  and the two trion lines  $X_T^-$  and  $X_S^-$ . The opposite slope means that the  $g$  factor of  $I_T^-$  is positive. We measure  $g_{I_T^-} = +15.4 \pm 0.1$  and find a similar value in the other measured device, shown in Fig. S1 of the Supplemental

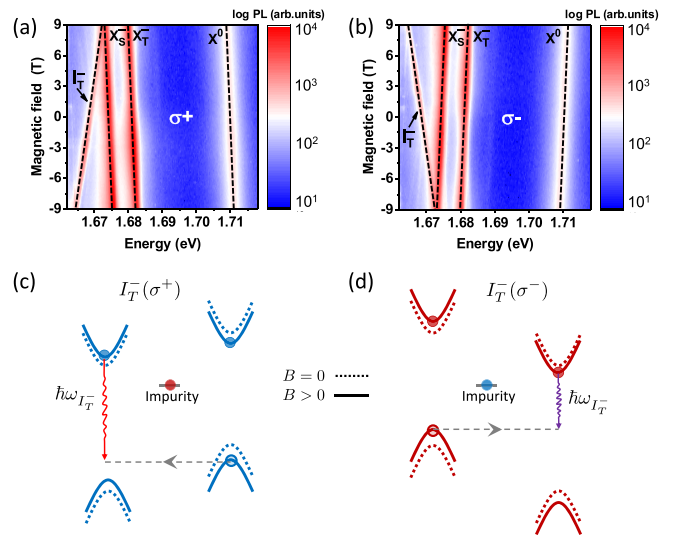


FIG. 3. Magnetic-field dependence of the luminescence in the  $\text{WSe}_2$  monolayer. The gate voltage is  $-2$  V, and the monolayer is excited by a linearly polarized laser. (a) and (b) The emitted light detected with  $\sigma^+$  and  $\sigma^-$  polarizations, respectively. (c) and (d) Schematics of the  $I_T^-$  transitions that correspond to emission with  $\sigma^\pm$  polarization. The dotted and solid lines correspond to energy bands at zero and positive magnetic fields, respectively.

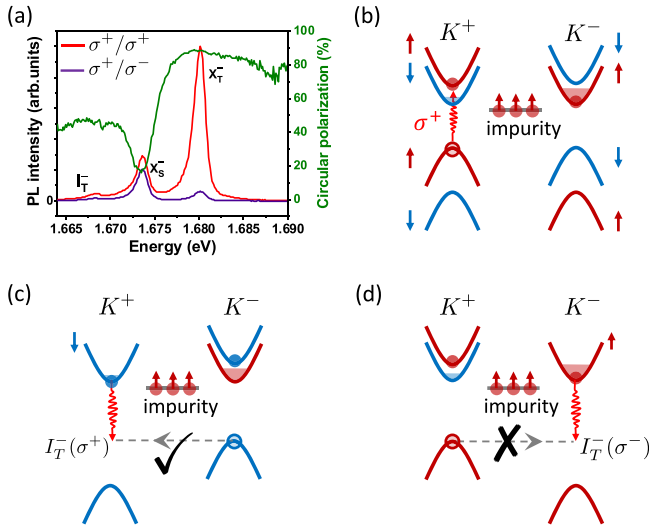


FIG. 4. Polarization analysis of the luminescence in the WSe<sub>2</sub> monolayer. The gate voltage is  $-2$  V, and the monolayer is excited by a  $\sigma^+$  polarized laser. (a) PL intensity detected with  $\sigma^+$  and  $\sigma^-$  polarizations. The green curve displays the corresponding circular polarization degree. (b) Schematics of the spin pumping process yielding a spin polarization of resident electrons in the CB valley at  $K^-$  and a simultaneous polarization of the impurity electron spin with the same orientation. (c) Due to Pauli exclusion, the short-range scattering of the trion off the impurity occurs only if the two electrons in the trion have spin opposite to that of the impurity electron. (d) The process is inefficient in the other case where the electrons of the trion and impurity have parallel spins. Here, the trion cannot approach the impurity close enough to facilitate intervalley transition of the hole.

Material [23]. Note that line  $I_T^-$  does not arise from the recombination of the intervalley dark trion recently identified in the WS<sub>2</sub> monolayer. As a matter of fact, it is also characterized by a negative  $g$  factor of about  $-14$ , the opposite of the positive  $g$  factor we measured in Fig. 3 [50]. The relatively large amplitude of the measured  $g$  factor indicates that the  $I_T^-$  transition is governed by indirect recombination of an electron in the bottom CB valley and a hole in the opposite top VB valley [22,24]. The positive sign of the  $g$  factor suggests that the hole experiences intervalley transition, as sketched in Fig. 2(b). The microscopic mechanism which allows the surprising observation of this normally forbidden transition will be detailed in the next section.

Finally, we present the circularly polarized luminescence following circularly polarized laser excitation at zero magnetic field. Figure 4(a) displays the luminescence polarization for singlet and triplet trions, as well as line  $I_T^-$ . As a consequence of very efficient spin pumping of resident electrons in the WSe<sub>2</sub> ML [21], the polarization of the triplet trion reaches very large values up to 80%. In addition, we observe that the polarization of the  $I_T^-$  component is also very large, typically 40% and copolarized with the laser.

### III. DISCUSSION

#### A. Impurity-assisted recombination of the triplet trion

We interpret the  $I_T^-$  transition as an impurity-assisted radiative recombination of the triplet trion. As we will show,

this mechanism is consistent with the different experimental signatures we described in the previous section. Despite the rather low number of studies on the influence of defects on the properties of TMDs, it is known that WSe<sub>2</sub> and WS<sub>2</sub> monolayers are characterized by a very large density of defects, typically,  $\sim 10^{12}$  cm<sup>-2</sup> [51–55]. It has also been shown that chalcogen vacancies induce a significant density of in-gap localized states close to the conduction band [56–58]. These defects induce a strong reduction of the luminescence yield at room temperature but also have some impacts on the recombination channels of certain exciton species. For instance, the zero-phonon indirect exciton transition has been clearly evidenced in the WSe<sub>2</sub> monolayer as a consequence of the recombination of an electron and a hole in opposite valleys [24]. In a way similar to the recombination of zero-phonon indirect transitions observed in semiconductors with impurities [59,60], the respective exciton transition in the WSe<sub>2</sub> ML is possible via impurity-assisted recombination, where the large wave-vector mismatch is accommodated by scattering off the short-range part of the impurity potential [28]. An impurity-assisted recombination of intervalley dark trion has also been observed in the WS<sub>2</sub> ML [50].

We argue that a similar impurity-assisted recombination process explains the origin of the emission from peak  $I_T^-$ . The initial state is the triplet trion, schematically shown in Fig. 2(a). It is composed of an electron and hole in the top CB and VB valleys at  $K^+$ , respectively, which are bound to an additional electron in the bottom CB valley at  $K^-$ . The photon emission associated with  $I_T^-$  is triggered by scattering of the triplet trion off the short-range impurity potential, during which the hole is virtually transitioned to the opposite valley at  $K^-$ , as shown schematically in Fig. 2(b). The transferred hole recombines with the resident electron in the opposite valley, emitting a photon with energy  $\hbar\omega_{I_T^-}$  and with circular polarization opposite to that of the direct recombination ( $X_T^-$ ). This recombination process can be described as a second-order transition, in which scattering of the triplet trion off the impurity induces a spin-conserving virtual intervalley transition of the hole from the top VB valley at  $K^+$  to the bottom VB valley at  $K^-$  (preserving its spin), followed by a virtual type-B optical transition. The transitions are virtual in the sense that the energy of the emitted photon is governed by the initial energy of the triplet and not by the energy gap of the type-B transition. Here, the role of elastic scattering off impurities during recombination is equivalent to the role of the exciton-phonon interaction when dealing with phonon-assisted recombination processes [24,61,62].

This interpretation is fully consistent with the magneto-PL results presented in Fig. 3 for linearly polarized laser excitation. We consider here the lowest energy transitions involving only the top VB, characterized by a  $g$  factor  $g_v$ . The bottom and top CB  $g$  factors are labeled  $g_{c1}$  and  $g_{c2}$ , respectively. The neutral exciton and trion  $g$  factors are simply written as  $g_{X^0} \approx g_{X_T^-} \approx g_{X_S^-} = -2(g_v - g_{c2})$ . The exciton  $g$  factors measured in Fig. 3 are in good agreement with the recently determined single-particle  $g$  factors of the top CB and VB valleys,  $g_{c2} = 3.84$  and  $g_v = 6.1$  (the  $g$  factor of the lowest CB is  $g_{c1} = 0.86$ ) [22].

The impurity-assisted recombination  $I_T^-$  of the triplet trion yields a large positive  $g$  factor as a consequence of the hole transfer to the opposite valley. Figures 3(c) and 3(d) show schematics of the CB and VB shifts considering a magnetic field  $B > 0$  for  $\sigma^+$  and  $\sigma^-$  polarized recombinations of  $I_T^-$ . One can readily check that the energies of these optical transitions are simply written as

$$E_{\sigma^\pm} = E_0 \pm (g_v + g_{c1})\mu_B B, \quad (1)$$

yielding a Zeeman splitting energy,

$$\Delta E = E_{\sigma^+} - E_{\sigma^-} = +2(g_v + g_{c1})\mu_B B. \quad (2)$$

Using measured single-particle  $g$  factors of the VB and CB [22], the  $g$  factor of the  $I_T^-$  transition is  $g_{I_T^-} \approx +13.7$ , which is only  $\sim 10\%$  smaller than the measured value ( $+15.4$ ). The impurity-assisted recombination of the triplet trion also explains very well the similar voltage dependences of the luminescence intensity of  $I_T^-$  and  $X_T^-$  in Fig. 1(d). The two lines correspond to two different recombination channels of the same triplet trion.

The Pauli exclusion principle plays a dual role in this impurity-assisted recombination process. First, the electrons of the triplet trion cannot go through a spin-conserving intervalley transition because a trion cannot have two electrons with the same spin and valley. Second, because the radiative process involves short-range scattering off the impurity, the electrons of the trion have to have spin opposite to that of the localized electron in the impurity, as shown in Fig. 2(c). This second feature can explain why the luminescence of the  $I_T^-$  line is copolarized with the laser if we now consider circularly polarized excitation, as in the experiment presented in Fig. 4. We explain this behavior as follows. As demonstrated in Ref. [21], the  $\sigma^+$  polarized excitation polarizes the resident electrons in the bottom CB valley at  $K^-$ . That is, it results in an imbalance between the population of resident electrons in the bottom CB valley at  $K^+$  and  $K^-$ , denoted by the shaded areas in Fig. 4(b). The spin pumping process is followed by polarization of the impurity level with spin similar to that of the polarized CB electrons. This kind of impurity spin pumping has been evidenced in various semiconductors [63–66]. The result is that the  $\sigma^+$  polarized laser yields a spin-up polarization of the impurities, as shown in Figs. 4(c) and 4(d). Assuming bimolecular formation of the trion from the neutral exciton, we have to consider the two configurations displayed in Figs. 4(c) and 4(d). These two configurations result from the fact that the neutral exciton polarization is modest (typically 20%, not shown) as a result of the very efficient exciton spin relaxation induced by the long-range electron-hole exchange interaction [67]. Due to Pauli exclusion, short-range scattering off the impurity occurs only in the configuration displayed in Fig. 4(c), where the two electron spins of the trion are opposite to the impurity's electron spin. Put differently, the spin-up polarized impurity interacts effectively only with triplet trions that have spin-down electrons. The result is  $\sigma^+$  polarized luminescence (i.e., copolarized with the laser), in agreement with the experimental results in Fig. 4(a). The scattering of the trion off the impurity with the other configuration, as shown in Fig. 4(d),

is inefficient since the two electrons of the trion have spins parallel to that of the impurity.

In summary, the interpretation of the  $I_T^-$  transition as an impurity-assisted radiative process of the triplet trion during which the hole recombines with the “wrong” electron, is consistent with all the experimental characteristics detailed in Sec. II.

(1) The emission appears when electrons are added to the ML, and its intensity increases in a way similar to the direct-gap emission from the triplet trion  $X_T^-$ .

(2) As expected from the second-order recombination process sketched in Fig. 2, the dipole transition is in plane polarized and not  $z$  polarized because it involves an optical transition between matching spin energy bands.

(3) The emission is characterized by a large positive  $g$  factor. The large value indicates that the recombination is across the indirect energy gap [24]. The positive value means that the hole experiences intervalley transition because the Pauli exclusion principle prevents the electrons of a triplet trion from going through an intervalley transition.

(4) Following circularly polarized excitation, the PL circular polarization is copolarized with that of the laser due to spin/valley pumping [21].

We can now understand why triplet and not singlet trions experience impurity-assisted recombination. Any valley switch in the singlet trion case ends up with the hole and electron in opposite valleys, which, consequently, cannot yield the emission of any photon. Finally, the screening of the impurity by a large density of free electrons can explain why the emission of  $I_T^-$  vanishes when the electron densities are larger than  $\sim 3 \times 10^{11} \text{ cm}^{-2}$ , in contrast to the direct transition of the triplet  $X_T^-$ , as shown in Fig. 1(b).

Alternative interpretations do not make it possible to explain all these experimental facts. For instance, of all phonon-assisted processes, only the  $K_1$  zone-edge phonon replica (18 meV) supports a valley change of the hole to provide a positive  $g$  factor, as measured previously for the neutral indirect exciton or the dark trion [24,28]. However, this process can be ruled out since no transition exists 18 meV above  $I_T^-$ , and furthermore, there should not be a decay of such phonon-assisted emission at larger electron densities. We could also think about a process based on the direct Coulomb interaction between the neutral indirect exciton and resident electrons; this would yield a hole valley change simultaneous with an electron valley change from the bottom to top CB valleys. This interpretation could explain the energy position of the  $I_T^-$  line and its positive  $g$  factor, yet it is unlikely for two reasons. First, the indirect exciton population is significant only in the neutral region, and it vanishes before peak  $I_T^-$  emerges [in a way similar to the behavior of the dark neutral exciton  $D^0$  in Fig. 1(d)]. Second, it was shown theoretically that in these TMD monolayers the exchange scattering is relatively strong despite the neutrality of the exciton, whereas the direct Coulomb scattering component is weak [8]. Finally, we believe that an inelastic scattering process in which the trion loses some of its kinetic energy to the screening electron cloud around the impurity can also be ruled out since the experiments are performed at very small charge densities (i.e., no electron screening cloud). Moreover, we show that

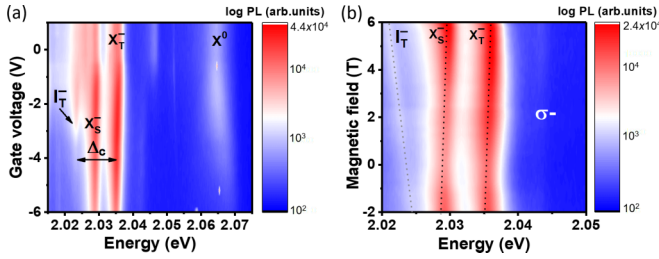


FIG. 5. (a) Photoluminescence intensity as a function of gate voltage in the WS<sub>2</sub> monolayer. (b) Magnetic-field dependence of the luminescence for  $\sigma^-$  detection, when the gate voltage is  $-3$  V. The excitation laser energy is  $2.33$  eV, and it is linearly polarized.

the impurity-assisted recombination effect decays when the screening becomes relevant.

### B. Measurement of the CB spin-orbit splitting in the WSe<sub>2</sub> ML

Compared with the much stronger direct-gap optical transition energy  $\hbar\omega_{X_T^-}$ , after which the left-behind electron is the one in the bottom CB valley at  $K^-$  [Fig. 2(a)], the left-behind electron in the impurity-assisted recombination process  $\hbar\omega_{I_T^-}$  is the top CB valley electron at  $K^+$  [Fig. 2(b)]. Thus, the energy difference between the emitted photons from the two possible recombination processes of the triplet trion is simply the CB spin-orbit splitting [see Figs. 1(b) and 1(c)]. We measure  $\Delta_c = 12 \pm 0.5$  meV. Note that the energy difference between the peaks of the triplet trion following regular and impurity-assisted recombination is consistent with the energy difference between the emission of dark trions and their brightened component [labeled  $D^-$  and  $D_{B^-}$  in Fig. 1(b)]. The brightening process of  $D^-$  resulting in  $D_{B^-}$  was described in Refs. [8,9]. In both cases, the energy difference is the CB spin-orbit splitting  $\Delta_c$ .

The value of  $\Delta_c$  we determine here is much smaller than the estimated value from measurements of Landau levels in WSe<sub>2</sub> monolayers ( $\sim 29$  meV) [16]. However, our measured value is consistent with the one estimated from the measurement of the Rydberg series of bright and dark excitons in WSe<sub>2</sub> MLs in a large in-plane magnetic field:  $\Delta_c \approx 14$  meV [15]. We emphasize that our measurement corresponds to the single-particle CB spin-orbit splitting; it is not influenced by band-gap renormalization effects due to exchange interactions, as our measurements are performed at relatively small electron densities, of the order of  $10^{11}$  cm<sup>-2</sup>.

### C. Impurity-assisted recombination of the triplet trion and CB spin-orbit splitting in the WS<sub>2</sub> ML

All the results presented so far were obtained for the WSe<sub>2</sub> ML. We have also investigated a charge adjustable device with a WS<sub>2</sub> ML following the exact same approach. As the results are very similar, we will not show all the data and comment only on the main experimental features. Figure 5(a) displays the PL intensity color plot as a function of applied

voltage in the charge tunable WS<sub>2</sub> device (Fig. S5 of the Supplemental Material shows the power dependence of the PL intensity [23]). Like for WSe<sub>2</sub>, we recognize the PL peaks associated with the recombination of the bright ( $X^0$ ) exciton, and when electrons are added to the ML, we recognize the emission from the singlet ( $X_S^-$ ) and triplet ( $X_T^-$ ) trions [50,68,69]. Remarkably, we also observe the  $I_T^-$  line, which has the same characteristics as the one evidenced in the WSe<sub>2</sub> ML. Following excitation by circularly polarized light, it is copolarized with the laser, and it has a large  $g$  factor,  $g_{I_T^-} = +14.6 \pm 0.9$ , with a sign opposite to the  $g$  factor of the trions,  $g_{X_T^-} = -3.5 \pm 0.5$  and  $g_{X_S^-} = -3.7 \pm 0.3$ , as shown in Fig. 5(b) [70–72]. Using the same reasoning as for WSe<sub>2</sub>, the measured difference between lines  $X_T^-$  and  $I_T^-$  yields the CB spin-orbit splitting in the WS<sub>2</sub> ML. We find  $\Delta_c = 12 \pm 1$  meV. The similar values of  $\Delta_c$  in both the WSe<sub>2</sub> and WS<sub>2</sub> MLs is corroborated by the similarity of other excitonic features (the slightly higher uncertainty for WS<sub>2</sub> is related to broader PL lines). For example, the neutral exciton bright-dark energy splitting is  $40$  meV in both hexagonal boron nitride encapsulated WSe<sub>2</sub> and WS<sub>2</sub> MLs [39,73].

## IV. SUMMARY

We have evidenced a line in the photoluminescence spectra of WSe<sub>2</sub> and WS<sub>2</sub> monolayers when a relatively small electron density is introduced. Our detailed characterizations allowed us to interpret this emission peak as being the result of an impurity-assisted recombination of the triplet trion. This identification yields a straightforward measurement of the single-particle conduction band spin-orbit splitting  $\Delta_c$ , which is simply the energy difference between the emission peaks of the triplet trion following regular and impurity-assisted recombinations. We found  $\Delta_c = 12 \pm 0.5$  meV for the WSe<sub>2</sub> monolayer and  $\Delta_c = 12 \pm 1$  meV for the WS<sub>2</sub> monolayer. Besides the measurement of conduction band spin-orbit splitting, which is key to understanding the properties of 2D materials based on transition-metal dichalcogenides, this work showed the importance of second-order recombination processes in WSe<sub>2</sub> or WS<sub>2</sub> monolayers. Phonon or impurity-assisted recombinations could also explain some transitions observed by photoluminescence spectroscopy in hetero- and homobilayers.

## ACKNOWLEDGMENTS

This work was supported by the Agence Nationale de la Recherche under the program ESR/EquipEx+ (Grant No. ANR-21-ESRE-0025) and ANR projects ATOEMS and Magicvalley. The work at the University of Rochester was supported by the Office of Naval Research (P.L.), under Contract No. N000142112448, and the Department of Energy, Basic Energy Sciences (D.V.T.), under Contract No. DE-SC0014349. The work at the University of Washington is supported by the Department of Energy, Basic Energy Sciences, under Award No. DE-SC0018171.

- [1] X. Xu, W. Yao, D. Xiao, and T. F. Heinz, Spin and pseudospins in layered transition-metal dichalcogenides, *Nat. Phys.* **10**, 343 (2014).
- [2] K. F. Mak and J. Shan, Photonics and optoelectronics of 2D semiconductor transition-metal dichalcogenides, *Nat. Photonics* **10**, 216 (2016).
- [3] G. Wang, A. Chernikov, M. M. Glazov, T. F. Heinz, X. Marie, T. Amand, and B. Urbaszek, Colloquium: Excitons in atomically thin transition-metal dichalcogenides, *Rev. Mod. Phys.* **90**, 021001 (2018).
- [4] D. M. Kennes, M. Claassen, L. Xian, A. Georges, A. J. Millis, J. Hone, C. R. Dean, D. N. Basov, A. N. Pasupathy, and A. Rubio, Moiré heterostructures as a condensed-matter quantum simulator, *Nat. Phys.* **17**, 155 (2021).
- [5] E. C. Regan, D. Wang, E. Y. Paik, Y. Zeng, L. Zhang, J. Zhu, A. H. MacDonald, H. Deng, and F. Wang, Emerging exciton physics in transition-metal dichalcogenide heterobilayers, *Nat. Rev. Mater.* **7**, 778 (2022).
- [6] D. Xiao, G.-B. Liu, W. Feng, X. Xu, and W. Yao, Coupled Spin and Valley Physics in Monolayers of MoS<sub>2</sub> and other Group-VI Dichalcogenides, *Phys. Rev. Lett.* **108**, 196802 (2012).
- [7] Y. Song and H. Dery, Transport Theory of Monolayer Transition-Metal Dichalcogenides through Symmetry, *Phys. Rev. Lett.* **111**, 026601 (2013).
- [8] M. Yang, L. Ren, C. Robert, D. V. Tuan, L. Lombez, B. Urbaszek, X. Marie, and H. Dery, Relaxation and darkening of excitonic complexes in electrostatically doped monolayer WSe<sub>2</sub>: Roles of exciton-electron and trion-electron interactions, *Phys. Rev. B* **105**, 085302 (2022).
- [9] D. V. Tuan, S.-F. Shi, X. Xu, S. A. Crooker, and H. Dery, Six-Body and Eight-Body Exciton States in Monolayer WSe<sub>2</sub>, *Phys. Rev. Lett.* **129**, 076801 (2022).
- [10] K. Kořmider, J. W. González, and J. Fernández-Rossier, Large spin splitting in the conduction band of transition metal dichalcogenide monolayers, *Phys. Rev. B* **88**, 245436 (2013).
- [11] A. Kormányos, G. Burkard, M. Gmitra, J. Fabian, V. Zólyomi, N. D. Drummond, and V. Fal'ko,  $\mathbf{k} \cdot \mathbf{p}$  theory for two-dimensional transition metal dichalcogenide semiconductors, *2D Mater.* **2**, 022001 (2015).
- [12] J. P. Echeverry, B. Urbaszek, T. Amand, X. Marie, and I. C. Gerber, Splitting between bright and dark excitons in transition metal dichalcogenide monolayers, *Phys. Rev. B* **93**, 121107(R) (2016).
- [13] D. Y. Qiu, T. Cao, and S. G. Louie, Nonanalyticity, Valley Quantum Phases, and Lightlike Exciton Dispersion in Monolayer Transition Metal Dichalcogenides: Theory and First-Principles Calculations, *Phys. Rev. Lett.* **115**, 176801 (2015).
- [14] C. Robert, B. Han, P. Kapuscinski, A. Delhomme, C. Faugeras, T. Amand, M. R. Molas, M. Bartos, K. Watanabe, T. Taniguchi, B. Urbaszek, M. Potemski, and X. Marie, Measurement of the spin-forbidden dark excitons in MoS<sub>2</sub> and MoSe<sub>2</sub> monolayers, *Nat. Commun.* **11**, 4037 (2020).
- [15] P. Kapuściński, A. Delhomme, D. Vaclavkova, A. O. Slobodeniuk, M. Grzeszczyk, M. Bartos, K. Watanabe, T. Taniguchi, C. Faugeras, and M. Potemski, Rydberg series of dark excitons and the conduction band spin-orbit splitting in monolayer WSe<sub>2</sub>, *Commun. Phys.* **4**, 186 (2021).
- [16] Z. Wang, J. Shan, and K. F. Mak, Valley- and spin-polarized Landau levels in monolayer WSe<sub>2</sub>, *Nat. Nanotechnol.* **12**, 144 (2017).
- [17] M. V. Gustafsson, M. Yankowitz, C. Forsythe, D. Rhodes, K. Watanabe, T. Taniguchi, J. Hone, X. Zhu, and C. R. Dean, Ambipolar Landau levels and strong band-selective carrier interactions in monolayer WSe<sub>2</sub>, *Nat. Mater.* **17**, 411 (2018).
- [18] R. Pisoni, A. Kormányos, M. Brooks, Z. Lei, P. Back, M. Eich, H. Overweg, Y. Lee, P. Rickhaus, K. Watanabe, T. Taniguchi, A. Imamoglu, G. Burkard, T. Ihn, and K. Ensslin, Interactions and Magnetotransport through Spin-Valley Coupled Landau Levels in Monolayer MoS<sub>2</sub>, *Phys. Rev. Lett.* **121**, 247701 (2018).
- [19] Y. Wang, T. Sohler, K. Watanabe, T. Taniguchi, M. J. Verstraete, and E. Tutuc, Electron mobility in monolayer WS<sub>2</sub> encapsulated in hexagonal boron-nitride, *Appl. Phys. Lett.* **118**, 102105 (2021).
- [20] S. Larentis, H. C. P. Movva, B. Fallahzad, K. Kim, A. Behroozi, T. Taniguchi, K. Watanabe, S. K. Banerjee, and E. Tutuc, Large effective mass and interaction-enhanced Zeeman splitting of *K*-valley electrons in MoSe<sub>2</sub>, *Phys. Rev. B* **97**, 201407(R) (2018).
- [21] C. Robert, S. Park, F. Cadiz, L. Lombez, L. Ren, H. Tornatzky, A. Rowe, D. Paget, F. Sirotti, M. Yang, D. V. Tuan, T. Taniguchi, B. Urbaszek, K. Watanabe, T. Amand, H. Dery, and X. Marie, Spin/valley pumping of resident electrons in WSe<sub>2</sub> and WS<sub>2</sub> monolayers, *Nat. Commun.* **12**, 5455 (2021).
- [22] C. Robert, H. Dery, L. Ren, D. Van Tuan, E. Courtade, M. Yang, B. Urbaszek, D. Lagarde, K. Watanabe, T. Taniguchi, T. Amand, and X. Marie, Measurement of Conduction and Valence Bands *g*-Factors in a Transition Metal Dichalcogenide Monolayer, *Phys. Rev. Lett.* **126**, 067403 (2021).
- [23] See Supplemental Material at <http://link.aps.org/supplemental/10.1103/PhysRevB.107.245407> for details on the magneto-PL measurement of  $I_T^-$  performed in a second WSe<sub>2</sub> device and measurements of the dipole orientation as well as power dependence in WSe<sub>2</sub> and WS<sub>2</sub> devices, which includes Refs. [74,75].
- [24] M. He, P. Rivera, D. V. Tuan, N. P. Wilson, M. Yang, T. Taniguchi, K. Watanabe, J. Yan, D. G. Mandrus, H. Yu, H. Dery, W. Yao, and X. Xu, Valley phonons and exciton complexes in a monolayer semiconductor, *Nat. Commun.* **11**, 618 (2020).
- [25] M. Sidler, P. Back, O. Cotlet, A. Srivastava, T. Fink, M. Kroner, E. Demler, and A. Imamoglu, Fermi polaron-polaritons in charge-tunable atomically thin semiconductors, *Nat. Phys.* **13**, 255 (2017).
- [26] M. M. Glazov, Optical properties of charged excitons in two-dimensional semiconductors, *J. Chem. Phys.* **153**, 034703 (2020).
- [27] T. Belhadj, C.-M. Simon, T. Amand, P. Renucci, B. Chatel, O. Krebs, A. Lemaitre, P. Voisin, X. Marie, and B. Urbaszek, Controlling the Polarization Eigenstate of a Quantum Dot Exciton with Light, *Phys. Rev. Lett.* **103**, 086601 (2009).
- [28] P. Li, C. Robert, D. Van Tuan, L. Ren, M. Yang, X. Marie, and H. Dery, Intervalley electron-hole exchange interaction and impurity-assisted recombination of indirect excitons in WS<sub>2</sub> and WSe<sub>2</sub> monolayers, *Phys. Rev. B* **106**, 085414 (2022).
- [29] A. M. Jones, H. Yu, J. Schaibley, J. Yan, D. G. Mandrus, T. Taniguchi, K. Watanabe, H. Dery, W. Yao, and X. Xu, Excitonic luminescence upconversion in a two-dimensional semiconductor, *Nat. Phys.* **12**, 323 (2016).
- [30] E. Courtade, M. Semina, M. Manca, M. M. Glazov, C. Robert, F. Cadiz, G. Wang, T. Taniguchi, K. Watanabe, M. Pierre, W. Escoffier, E. L. Ivchenko, P. Renucci, X. Marie, T. Amand, and

- B. Urbaszek, Charged excitons in monolayer WSe<sub>2</sub>: Experiment and theory, *Phys. Rev. B* **96**, 085302 (2017).
- [31] Z. Li, T. Wang, S. Miao, Z. Lian, and S.-F. Shi, Fine structures of valley-polarized excitonic states in monolayer transitional-metal dichalcogenides, *Nanophotonics* **9**, 1811 (2020).
- [32] E. Liu, J. van Baren, Z. Lu, M. M. Altairy, T. Taniguchi, K. Watanabe, D. Smirnov, and C. H. Lui, Gate Tunable Dark Triions in Monolayer WSe<sub>2</sub>, *Phys. Rev. Lett.* **123**, 027401 (2019).
- [33] Z. Li, T. Wang, Z. Lu, M. Khatoniari, Z. Lian, Y. Meng, M. Blei, T. Taniguchi, K. Watanabe, S. A. McGill, S. Tongay, V. M. Menon, D. Smirnov, and S.-F. Shi, Direct observation of gate-tunable dark triions in monolayer WSe<sub>2</sub>, *Nano Lett.* **19**, 6886 (2019).
- [34] E. Liu, J. van Baren, C.-T. Liang, T. Taniguchi, K. Watanabe, N. M. Gabor, Y.-C. Chang, and C.-H. Lui, Multipath Optical Recombination of Intervalley Dark Excitons and Triions in Monolayer WSe<sub>2</sub>, *Phys. Rev. Lett.* **124**, 196802 (2020).
- [35] M. Barbone, A. R.-P. Montblanch, D. M. Kara, C. Palacios-Berraquero, A. R. Cadore, D. De Fazio, B. Pingault, E. Mostaani, H. Li, B. Chen, K. Watanabe, T. Taniguchi, S. Tongay, G. Wang, A. C. Ferrari, and M. Atatüre, Charge-tunable biexciton complexes in monolayer WSe<sub>2</sub>, *Nat. Commun.* **9**, 3721 (2018).
- [36] A. Srivastava, M. Sidler, A. V. Allain, D. S. Lembke, A. Kis, and A. Imamoglu, Optically active quantum dots in monolayer WSe<sub>2</sub>, *Nat. Nanotechnol.* **10**, 491 (2015).
- [37] Y.-M. He, G. Clark, J. R. Schaibley, Y. He, M.-C. Chen, Y.-J. Wei, X. Ding, Q. Zhang, W. Yao, X. Xu, C.-Y. Lu, and J.-W. Pan, Single quantum emitters in monolayer semiconductors, *Nat. Nanotechnol.* **10**, 497 (2015).
- [38] M. Koperski, K. Nogajewski, A. Arora, V. Cherkez, P. Mallet, J.-Y. Veuillen, J. Marcus, P. Kossacki, and M. Potemski, Single photon emitters in exfoliated WSe<sub>2</sub> structures, *Nat. Nanotechnol.* **10**, 503 (2015).
- [39] G. Wang, C. Robert, M. M. Glazov, F. Cadiz, E. Courtade, T. Amand, D. Lagarde, T. Taniguchi, K. Watanabe, B. Urbaszek, and X. Marie, In-Plane Propagation of Light in Transition Metal Dichalcogenide Monolayers: Optical Selection Rules, *Phys. Rev. Lett.* **119**, 047401 (2017).
- [40] G. Sallen, L. Bouet, X. Marie, G. Wang, C. R. Zhu, W. P. Han, Y. Lu, P. H. Tan, T. Amand, B. L. Liu, and B. Urbaszek, Robust optical emission polarization in MoS<sub>2</sub> monolayers through selective valley excitation, *Phys. Rev. B* **86**, 081301(R) (2012).
- [41] K. F. Mak, K. L. He, J. Shan, and T. F. Heinz, Control of valley polarization in monolayer MoS<sub>2</sub> by optical helicity, *Nat. Nanotechnol.* **7**, 494 (2012).
- [42] T. Cao, G. Wang, W. Han, H. Ye, C. Zhu, J. Shi, Q. Niu, P. Tan, E. Wang, B. Liu, and J. Feng, Valley-selective circular dichroism of monolayer molybdenum disulfide, *Nat. Commun.* **3**, 887 (2012).
- [43] G. Kioseoglou, A. T. Hanbicki, M. Currie, A. L. Friedman, D. Gunlycke, and B. T. Jonker, Valley polarization and intervalley scattering in monolayer MoS<sub>2</sub>, *Appl. Phys. Lett.* **101**, 221907 (2012).
- [44] G. Wang, L. Bouet, M. M. Glazov, T. Amand, E. L. Ivchenko, E. Palleau, X. Marie, and B. Urbaszek, Magneto-optics in transition-metal diselenide monolayers, *2D Mater.* **2**, 034002 (2015).
- [45] G. Aivazian, Z. Gong, A. M. Jones, R.-L. Chu, J. Yan, D. G. Mandrus, C. Zhang, D. Cobden, W. Yao, and X. Xu, Magnetic control of valley pseudospin in monolayer WSe<sub>2</sub>, *Nat. Phys.* **11**, 148 (2015).
- [46] A. Srivastava, M. Sidler, A. V. Allain, D. S. Lembke, A. Kis, and A. Imamoglu, Valley Zeeman effect in elementary optical excitations of monolayer WSe<sub>2</sub>, *Nat. Phys.* **11**, 141 (2015).
- [47] C. Robert, T. Amand, F. Cadiz, D. Lagarde, E. Courtade, M. Manca, T. Taniguchi, K. Watanabe, B. Urbaszek, and X. Marie, Fine structure and lifetime of dark excitons in transition metal dichalcogenide monolayers, *Phys. Rev. B* **96**, 155423 (2017).
- [48] M. R. Molas, A. O. Slobodeniuk, T. Kazimierzczuk, K. Nogajewski, M. Bartos, P. Kapuscinski, K. Oreszczuk, K. Watanabe, T. Taniguchi, C. Faugeras, P. Kossacki, D. M. Basko, and M. Potemski, Probing and Manipulating Valley Coherence of Dark Excitons in Monolayer WSe<sub>2</sub>, *Phys. Rev. Lett.* **123**, 096803 (2019).
- [49] J. Förste, N. V. Tepliakov, S. Y. Kruchinin, J. Lindlau, V. Funk, M. Förg, K. Watanabe, T. Taniguchi, A. S. Baimuratov, and A. Högele, Exciton *g*-factors in monolayer and bilayer WSe<sub>2</sub> from experiment and theory, *Nat. Commun.* **11**, 4539 (2020).
- [50] M. Zinkiewicz, T. Woźniak, T. Kazimierzczuk, P. Kapuscinski, K. Oreszczuk, M. Grzeszczyk, M. Bartos, K. Nogajewski, K. Watanabe, T. Taniguchi, C. Faugeras, P. Kossacki, M. Potemski, A. Babiński, and M. R. Molas, Excitonic complexes in n-doped WS<sub>2</sub> monolayer, *Nano Lett.* **21**, 2519 (2021).
- [51] M. R. Molas, K. Nogajewski, A. O. Slobodeniuk, J. Binder, M. Bartos, and M. Potemski, The optical response of monolayer, few-layer and bulk tungsten disulfide, *Nanoscale* **9**, 13128 (2017).
- [52] D. Edelberg, D. Rhodes, A. Kerelsky, B. Kim, J. Wang, A. Zangiabadi, C. Kim, A. Abhinandan, J. Ardelean, M. Scully, D. Scullion, L. Embon, R. Zu, E. J. G. Santos, L. Balicas, C. Marianetti, K. Barmak, X. Zhu, J. Hone, and A. N. Pasupathy, Approaching the intrinsic limit in transition-metal diselenides via point defect control, *Nano Lett.* **19**, 4371 (2019).
- [53] A. Neumann, J. Lindlau, M. Nutz, A. D. Mohite, H. Yamaguchi, and A. Högele, Signatures of defect-localized charged excitons in the photoluminescence of monolayer molybdenum disulfide, *Phys. Rev. Mater.* **2**, 124003 (2018).
- [54] D. Rhodes, S. H. Chae, R. Ribeiro-Palau, and J. Hone, Disorder in van der Waals heterostructures of 2D materials, *Nat. Mater.* **18**, 541 (2019).
- [55] W. Murray, M. Lucking, E. Kahn, T. Zhang, K. Fujisawa, N. Perea-Lopez, A. L. Elias, H. Terrones, M. Terrones, and Z. Liu, Second harmonic generation in two-dimensional transition metal dichalcogenides with growth and post-synthesis defects, *2D Mater.* **7**, 045020 (2020).
- [56] S. Refaely-Abramson, D. Y. Qiu, S. G. Louie, and J. B. Neaton, Defect-Induced Modification of Low-Lying Excitons and Valley Selectivity in Monolayer Transition Metal Dichalcogenides, *Phys. Rev. Lett.* **121**, 167402 (2018).
- [57] H. Bretscher, Z. Li, J. Xiao, D. Y. Qiu, S. Refaely-Abramson, J. A. Alexander-Webber, A. Tanoh, Y. Fan, G. Delport, C. A. Williams, S. D. Stranks, S. Hofmann, J. B. Neaton, S. G. Louie, and A. Rao, Rational passivation of sulfur vacancy defects in two-dimensional transition metal dichalcogenides, *ACS Nano* **15**, 8780 (2021).
- [58] P. Rivera, M. He, B. Kim, S. Liu, C. Rubio-Verdú, H. Moon, L. Menzel, D. A. Rhodes, H. Yu, T. Taniguchi, K. Watanabe, J. Yan, D. G. Mandrus, H. Dery, A. Pasupathy, D. Englund, J. Hone, W. Yao, and X. Xu, Intrinsic donor-bound excitons in



- ultraclean monolayer semiconductors, *Nat. Commun.* **12**, 871 (2021).
- [59] M. Tajima, Determination of boron and phosphorus concentration in silicon by photoluminescence analysis, *Appl. Phys. Lett.* **32**, 719 (1978).
- [60] J. Wagner, Heavily doped silicon studied by luminescence and selective absorption, *Solid-State Electron.* **28**, 25 (1985).
- [61] H. Dery and Y. Song, Polarization analysis of excitons in monolayer and bilayer transition-metal dichalcogenides, *Phys. Rev. B* **92**, 125431 (2015).
- [62] D. Van Tuan, A. M. Jones, M. Yang, X. Xu, and H. Dery, Virtual Trions in the Photoluminescence of Monolayer Transition-Metal Dichalcogenides, *Phys. Rev. Lett.* **122**, 217401 (2019).
- [63] V. L. Berkovits, A. I. Ekimov, and V. I. Safarov, Optical orientation in a system of electrons and lattice nuclei in semiconductors. Experiment, *Sov. Phys. JETP* **38**, 169 (1974).
- [64] M. I. D'yakonov and V. I. Perel, Optical orientation in a system of electrons and lattice nuclei in semiconductors. Theory, *Sov. Phys. JETP* **38**, 177 (1974).
- [65] Q. Liu, C.-X. Liu, C. Xu, X.-L. Qi, and S.-C. Zhang, Magnetic Impurities on the Surface of a Topological Insulator, *Phys. Rev. Lett.* **102**, 156603 (2009).
- [66] L. Qing, J. Li, I. Appelbaum, and H. Dery, Spin relaxation via exchange with donor impurity-bound electrons, *Phys. Rev. B* **91**, 241405(R) (2015).
- [67] C. R. Zhu, K. Zhang, M. Glazov, B. Urbaszek, T. Amand, Z. W. Ji, B. L. Liu, and X. Marie, Exciton valley dynamics probed by Kerr rotation in WSe<sub>2</sub> monolayers, *Phys. Rev. B* **90**, 161302(R) (2014).
- [68] D. Vaclavkova, J. Wyzula, K. Nogajewski, M. Bartos, A. O. Slobodeniuk, C. Faugeras, M. Potemski, and M. R. Molas, Singlet and triplet trions in WS<sub>2</sub> monolayer encapsulated in hexagonal boron nitride, *Nanotechnology* **29**, 325705 (2018).
- [69] A. Arora, N. K. Wessling, T. Deilmann, T. Reichenauer, P. Steeger, P. Kossacki, M. Potemski, S. Michaelis de Vasconcellos, M. Rohlfing, and R. Bratschitsch, Dark trions govern the temperature-dependent optical absorption and emission of doped atomically thin semiconductors, *Phys. Rev. B* **101**, 241413(R) (2020).
- [70] R. Schmidt, A. Arora, G. Plechinger, P. Nagler, A. Granados del Aguila, M. V. Ballottin, P. C. M. Christianen, S. M. de Vasconcellos, C. Schüller, T. Korn, and R. Bratschitsch, Magnetic-Field-Induced Rotation of Polarized Light Emission from Monolayer WS<sub>2</sub>, *Phys. Rev. Lett.* **117**, 077402 (2016).
- [71] P. Nagler, M. V. Ballottin, A. A. Mitioglu, M. V. Durnev, T. Taniguchi, K. Watanabe, A. Chernikov, C. Schüller, M. M. Glazov, P. C. M. Christianen, and T. Korn, Zeeman Splitting and Inverted Polarization of Biexciton Emission in Monolayer WS<sub>2</sub>, *Phys. Rev. Lett.* **121**, 057402 (2018).
- [72] M. Koperski, M. R. Molas, A. Arora, K. Nogajewski, M. Bartos, J. Wyzula, D. Vaclavkova, P. Kossacki, and M. Potemski, Orbital, spin and valley contributions to Zeeman splitting of excitonic resonances in MoSe<sub>2</sub>, WSe<sub>2</sub> and WS<sub>2</sub> monolayers, *2D Mater.* **6**, 015001 (2018).
- [73] M. Zinkiewicz, A. O. Slobodeniuk, T. Kazimierzczuk, P. Kapuściński, K. Oreszczuk, M. Grzeszczyk, M. Bartos, K. Nogajewski, K. Watanabe, T. Taniguchi, C. Faugeras, P. Kossacki, M. Potemski, A. Babiński, and M. R. Molas, Neutral and charged dark excitons in monolayer WS<sub>2</sub>, *Nanoscale* **12**, 18153 (2020).
- [74] Z. Wang, L. Zhao, K. F. Mak, and J. Shan, Probing the spin-polarized electronic band structure in monolayer transition metal dichalcogenides by optical spectroscopy, *Nano Lett.* **17**, 740 (2017).
- [75] J. Li, M. Goryca, K. Yumigeta, H. Li, S. Tongay, and S. A. Crooker, Valley relaxation of resident electrons and holes in a monolayer semiconductor: Dependence on carrier density and the role of substrate-induced disorder, *Phys. Rev. Mater.* **5**, 044001 (2021).